

# Effects of Thermophoresis, Dufour, Hall and Radiation on an Unsteady MHD flow past an Inclined Plate with Viscous Dissipation

N. Pandya and A. K. Shukla

**Abstract**—The aim of this paper is to study the effects of Thermophoresis, Dufour, Hall and radiation on an unsteady MHD (Magnetohydro Dynamics) flow of a viscous incompressible fluid past an inclined porous plate embedded in porous medium. Partial differential equations of non-dimensional form of governing equations of flow have been solved numerically using Crank-Nicolson implicit finite difference method. The effects of different physical parameters on velocity, temperature and concentration profiles are discussed with graphs and numerical values of skin friction coefficients, Nusselt number and Sherwood number are discussed with tables.

**Index Terms**—MHD, Thermophoresis effect, Dufour effect, porous medium, Hall effect, radiation effect, Heat and Mass transfer, Crank-Nicolson method.

**MSC 2010 Codes** – 76W05, 76R50, 78A40 and 76M20.

## I. INTRODUCTION

**D**URING the last many decades, large number of mathematician has attraction toward study of unsteady MHD flow with effects of Thermophoresis, Dufour, radiation and Hall because of a large number of avenues for research work. The investigation of behavior of such flow have application in chemical engineering, MHD generators, in design of underground water energy storage system, soil sciences, nuclear power reactors, aeronautics and so on. MHD convection flow past a semi-infinite vertical plate with thermal radiation was discussed by Venkataramana [1]. Sparrow and Cess [2] have discussed the effect of magnetic field on free convection heat transfer. Effect of magnetic file on heat and mass transfer by natural convection from vertical surface in porous medium with Soret and Dufour effects was discussed by Postelnicu [3].

Rajesh et al. [4] studied effects of radiation and mass transfer on MHD flow with exponentially accelerated vertical plate. Interaction of mixed convection with thermal radiation in laminar flow had been analyzed by Bestman et al. [5]. Olanrewaju [6] discussed Soret-Dufour and radiation effects on transient free convection flow past a moving plate. Sudhakarraiah et al. [7] examined Soret effect on unsteady MHD flow past a vertical plate with heat source. Ghosh [8] studied effect of

Hall current on MHD flow in rotating system with arbitrary magnetic field. Hall effect on unsteady Couette flow have been studied by Jana et al. [9].

The aim of this research work is to examine combined effects of Soret or Thermophoresis, Dufour, Hall and radiation on unsteady MHD flow past an inclined porous plate embedded in porous medium along with viscous dissipation, variable temperature and variable mass diffusion. Partial differential equations of dimensionless governing equations of flow have been solved by Crank-Nicolson implicit finite difference method. Effects of different physical parameters of flow field on velocity, temperature, concentration, coefficients of skin-friction, Nusselt number and Sherwood number have been discussed through graphs and tables.

## II. MATHEMATICAL ANALYSIS

An unsteady MHD flow of a viscous incompressible fluid past an infinite inclined plate with variable temperature and mass diffusion with viscous dissipation has been analyzed. The plate is inclined at angle  $\lambda$  to vertical and embedded in porous medium.  $x'$ -axis has been considered along plate,  $y'$ -axis normal to it. Assumed  $z'$ -axis normal to  $x'y'$ -plane. A uniform magnetic field  $B_0$  is taken along  $y'$ -axis and plate is electrically non-conducting. Magnetic Reynolds number and transversely applied magnetic file are very small so induced magnetic field is negligible in comparison to applied magnetic field, Cowling [10].

$$\begin{aligned} J'_x &= \frac{\sigma B_0}{1+m^2}(mu' - w') \\ J'_z &= \frac{\sigma B_0}{1+m^2}(u' + mw') \end{aligned} \quad (1)$$

Where  $m$  is hall parameter,  $u'$  and  $w'$  are velocities,  $J'_x$  and  $J'_z$  are electric current density along  $x'$ -axis and  $z'$ -axis respectively.

Due to infinite length in  $x'$  direction, flow variables are function of  $t'$  and  $y'$  only. Consider usual Boussinesq approximation, governing equations of flow field are:

$$\frac{\partial v'}{\partial y'} = 0 \Rightarrow v' = -v_0(\text{constant}) \quad (2)$$

N. Pandya is with the Department of Mathematics and Astronomy, Lucknow University, Lucknow - 226007, U. P., India. (phone: +91-9450397558; E-mail: dr.nidh23@gmail.com)

A. K. Shukla is with the Department of Mathematics and Astronomy, Lucknow University, Lucknow - 226007, U. P., India. (phone: +91-9044158184; E-mail: ashishshukla1987@gmail.com).

$$\frac{\partial u'}{\partial t'} + v' \frac{\partial u'}{\partial y'} = \nu \frac{\partial^2 u'}{\partial y'^2} + g\gamma(T' - T'_\infty) \cos(\lambda) + g\gamma^*(C' - C'_\infty) \cos(\lambda) - \frac{\sigma B_0^2}{\rho(1+m^2)}(u' + mw') - \frac{\nu u'}{K'} \quad (3)$$

$$\frac{\partial w'}{\partial t'} + v' \frac{\partial w'}{\partial y'} = \nu \frac{\partial^2 w'}{\partial y'^2} + \frac{\sigma B_0^2}{\rho(1+m^2)}(mw' - w') - \frac{\nu w'}{K'} \quad (4)$$

$$\rho C_p \left( \frac{\partial T'}{\partial t'} + v' \frac{\partial T'}{\partial y'} \right) = k \frac{\partial^2 T'}{\partial y'^2} - \frac{\partial q_r}{\partial y'} + \frac{\rho D_m K_T}{c_s} \frac{\partial^2 C'}{\partial y'^2} + \mu \left( \frac{\partial u'}{\partial y'} \right)^2 \quad (5)$$

$$\frac{\partial C'}{\partial t'} + v' \frac{\partial C'}{\partial y'} = D \frac{\partial^2 C'}{\partial y'^2} + \frac{D_m K_T}{T_m} \frac{\partial^2 T'}{\partial y'^2} \quad (6)$$

where  $\gamma^*$  is coefficient of volume expansion for mass transfer,  $\gamma$  is volumetric coefficient of thermal expansion,  $v'$  is velocity along  $y'$ -axis,  $K$  is permeability of porous medium,  $\sigma$  is electrical conductivity,  $D_m$  is molecular diffusivity,  $g$  is acceleration due to gravity,  $K_T$  is thermal diffusion ratio,  $\mu$  is viscosity,  $\rho$  is fluid density,  $k$  is thermal conductivity of fluid,  $C'$  and  $T'$  are dimensional concentration and temperature,  $C'_\infty$  and  $T'_\infty$  are concentration and temperature of free stream,  $q_r$  is radiative heat along  $y'$ -axis,  $\nu$  is kinematic viscosity and  $T_m$  is mean fluid temperature.

Boundary and initial conditional for this model are given as:

$$\begin{aligned} t' \leq 0 \quad u' = 0 \quad w' = 0 \\ T' = T'_\infty \quad C' = C'_\infty \quad \forall y' \\ t' > 0 \quad u' = u_0 \quad v' = -v_0 \quad w' = 0 \\ T' = T'_\infty + (T'_w - T'_\infty)e^{Bt'}, \\ C' = C'_\infty + (C'_w - C'_\infty)e^{Bt'} \quad \text{at } y' = 0 \\ u' = 0 \quad w' = 0 \quad T' \rightarrow T'_\infty \quad C' \rightarrow C'_\infty \quad y' \rightarrow \infty \end{aligned} \quad (7)$$

where  $T'_w$  and  $C'_w$  are concentration and temperature respectively of plate and  $B = \frac{v_0^2}{\nu}$ .

$$q_r = -\frac{4\sigma}{3k_m} \frac{\partial T'^4}{\partial y'} \quad (8)$$

where  $\sigma$  and  $k_m$  are Stefan Boltzmann constant and mean absorption coefficient respectively. in this model temperature difference within flow is very small, so that  $T'^4$  may be expressed linearly with temperature. It is observed by expanding in a Taylor's series about  $T'_\infty$  and considering negligible higher order term, hence

$$T'^4 \cong 4T'^3_\infty T' - 3T'^4_\infty \quad (9)$$

so, by equations 8 and 9, equation 5 is reduced

$$\rho C_p \left( \frac{\partial T'}{\partial t'} + v' \frac{\partial T'}{\partial y'} \right) = k \frac{\partial^2 T'}{\partial y'^2} + \frac{16\sigma T'^3_\infty}{3k_m} \frac{\partial^2 T'}{\partial y'^2} + \frac{\rho D_m K_T}{c_s} \frac{\partial^2 C'}{\partial y'^2} + \mu \left( \frac{\partial u'}{\partial y'} \right)^2 \quad (10)$$

In order to obtain dimensionless partial differential equations, we introduce following quantities:

$$\begin{aligned} u = \frac{u'}{u_0}, \quad t = \frac{t'v_0^2}{\nu}, \quad \theta = \frac{T' - T'_\infty}{T'_w - T'_\infty}, \\ C = \frac{C' - C'_\infty}{C'_w - C'_\infty}, \quad Gm = \frac{\nu g \alpha^* (C'_w - C'_\infty)}{u_0 v_0^2}, \\ Gr = \frac{\nu g \alpha (T'_w - T'_\infty)}{u_0 v_0^2}, \quad Du = \frac{D_m K_T (C'_w - C'_\infty)}{c_s c_p \nu (T'_w - T'_\infty)}, \\ Sr = \frac{D_m K_T (T'_w - T'_\infty)}{T_m \nu (C'_w - C'_\infty)}, \\ K = \frac{v_0^2 K'}{\nu^2}, \quad Pr = \frac{\mu c_p}{k}, \quad M = \frac{\sigma B_0^2 \nu}{\rho v_0^2}, \\ R = \frac{4\sigma T'^3_\infty}{k_m k}, \quad Sc = \frac{\nu}{D_m}, \quad y = \frac{y' v_0}{\nu}, \\ w = \frac{w'}{u_0}, \quad Ec = \frac{u_0^2}{c_p (T'_w - T'_\infty)} \end{aligned} \quad (11)$$

Using quantities of equation 11, we get non-dimensional form of equations 3, 4, 10 and 6 respectively:

$$\frac{\partial u}{\partial t} - \frac{\partial u}{\partial y} = \frac{\partial^2 u}{\partial y^2} + Gr \cos(\lambda) \theta + Gm \cos(\lambda) C - \left( \frac{M}{1+m^2} + \frac{1}{K} \right) u - \left( \frac{mM}{1+m^2} \right) w \quad (12)$$

$$\frac{\partial w}{\partial t} - \frac{\partial w}{\partial y} = \frac{\partial^2 w}{\partial y^2} - \left( \frac{M}{1+m^2} + \frac{1}{K} \right) w + \left( \frac{mM}{1+m^2} \right) u \quad (13)$$

$$\frac{\partial \theta}{\partial t} - \frac{\partial \theta}{\partial y} = \frac{1}{Pr} \left( 1 + \frac{4R}{3} \right) \frac{\partial^2 \theta}{\partial y^2} + Du \frac{\partial^2 C}{\partial y^2} + Ec \left( \frac{\partial u}{\partial y} \right)^2 \quad (14)$$

$$\frac{\partial C}{\partial t} - \frac{\partial C}{\partial y} = \frac{1}{Sc} \frac{\partial^2 C}{\partial y^2} + Sr \frac{\partial^2 \theta}{\partial y^2} \quad (15)$$

dimensionless boundary and initial conditions are::

$$\begin{aligned} t \leq 0 \quad u = 0 \quad w = 0 \quad \theta = 0 \quad C = 0 \quad \forall y \\ t > 0 \quad u = 1 \quad w = 0 \quad \theta = e^t \quad C = e^t \quad \text{at } y = 0 \\ u = 0 \quad w = 0 \quad \theta \rightarrow 0 \quad C \rightarrow 0 \quad y \rightarrow \infty \end{aligned} \quad (16)$$

Further, there is primary interest for research workers to calculate physical quantities skin-friction coefficients  $\tau_1$  and  $\tau_2$  along wall  $x$ -axis and  $z$ -axis respectively, Nusselt number  $Nu$  and Sherwood number  $Sh$ . Non-dimensional form of these physical quantities are:

$$\begin{aligned} \tau_1 &= \left( \frac{\partial u}{\partial y} \right)_{y=0} \\ \tau_2 &= \left( \frac{\partial w}{\partial y} \right)_{y=0} \\ Nu &= - \left( \frac{\partial \theta}{\partial y} \right)_{y=0} \\ Sh &= - \left( \frac{\partial C}{\partial y} \right)_{y=0} \end{aligned} \quad (17)$$

### III. METHOD OF SOLUTION

Partial differential equations 12 to 15 are solved with initial and boundary conditions 16. To find exact solution of these partial differential equations are impossible. So, these are solved numerically using Crank-Nicolson implicit finite difference method. First, equations 12, 13, 14 and 15 are expressed as:

$$\begin{aligned} & \frac{u_{i,j+1} - u_{i,j}}{\Delta t} - \frac{u_{i+1,j} - u_{i,j}}{\Delta y} = \\ & \left( \frac{u_{i-1,j} - 2u_{i,j} + u_{i-1,j} - 2u_{i,j+1} + u_{i+1,j+1}}{2(\Delta y)^2} \right) \\ & + Gr \cos(\lambda) \left( \frac{\theta_{i,j+1} - \theta_{i,j}}{2} \right) \\ & + Gm \cos(\lambda) \left( \frac{C_{i,j} + 1 - C_{i,j}}{2} \right) \end{aligned} \quad (18)$$

$$\begin{aligned} & - \left( \frac{M}{1+m^2} + \frac{1}{K} \right) \left( \frac{u_{i,j+1} + u_{i,j}}{2} \right) \\ & - \left( \frac{mM}{1+m^2} \right) \left( \frac{w_{i,j+1} + w_{i,j}}{2} \right) \\ & \frac{w_{i,j+1} - w_{i,j}}{\Delta t} - \frac{w_{i+1,j} - w_{i,j}}{\Delta y} = \\ & \left( \frac{w_{i-1,j} - 2w_{i,j} + w_{i-1,j} - 2w_{i,j+1} + w_{i+1,j+1}}{2(\Delta y)^2} \right) \\ & - \left( \frac{M}{1+m^2} + \frac{1}{K} \right) \left( \frac{uw_{i,j+1} + w_{i,j}}{2} \right) \\ & + \left( \frac{mM}{1+m^2} \right) \left( \frac{u_{i,j+1} + u_{i,j}}{2} \right) \end{aligned} \quad (19)$$

$$\begin{aligned} & \frac{\theta_{i,j+1} - \theta_{i,j}}{\Delta t} - \frac{\theta_{i+1,j} - \theta_{i,j}}{\Delta y} = \\ & \left( \frac{1}{Pr} + \frac{4R}{3Pr} \right) \\ & \left( \frac{\theta_{i-1,j} - 2\theta_{i,j} + \theta_{i-1,j} - 2\theta_{i,j+1} + \theta_{i+1,j+1}}{2(\Delta y)^2} \right) \\ & + Du \left( \frac{C_{i-1,j} - 2u_{i,j} + C_{i-1,j} - 2C_{i,j+1} + C_{i+1,j+1}}{2(\Delta y)^2} \right) \\ & + Ec \left( \frac{u_{i+1,j} - u_{i,j}}{\Delta y} \right)^2 \end{aligned} \quad (20)$$

$$\begin{aligned} & \frac{C_{i,j+1} - C_{i,j}}{\Delta t} - \frac{C_{i+1,j} - C_{i,j}}{\Delta y} = \\ & \frac{1}{Sc} \left( \frac{C_{i-1,j} - 2u_{i,j} + C_{i-1,j} - 2C_{i,j+1} + C_{i+1,j+1}}{2(\Delta y)^2} \right) \\ & + Sr \left( \frac{\theta_{i-1,j} - 2\theta_{i,j} + \theta_{i-1,j} - 2\theta_{i,j+1} + \theta_{i+1,j+1}}{2(\Delta y)^2} \right) \end{aligned} \quad (21)$$

initial and boundary conditions are also expressed as:

$$\begin{aligned} & u_{i,0} = 0 \quad w_{i,0} = 0 \quad \theta_{i,0} = 0 \quad C_{i,0} = 0 \quad \forall i \\ & u_{0,j} = 1 \quad w_{0,j} = 0 \quad \theta_{0,j} = e^{j\Delta t} \quad C_{0,j} = e^{j\Delta t} \\ & u_{X,j} = 0 \quad w_{X,j} = 0 \quad \theta_{X,j} \rightarrow 0 \quad C_{X,j} \rightarrow 0 \end{aligned} \quad (22)$$

where index  $i$  refers to  $y$ ,  $j$  refers to time  $t$ ,  $\Delta t = t_{j+1} - t_j$  and  $\Delta y = y_{i+1} - y_i$ . Known values of  $u$ ,  $w$ ,  $\theta$  and  $C$  at  $t$ , we solved above equations for values  $t + \Delta t$  as follows: We

obtain these values to substitute  $i = 1, 2, 3, \dots, X - 1$ , where  $X$  pertains to  $\infty$  then equations 18 to 21 give tridiagonal system of equations with initial and boundary conditions in equation 22 are solved using Thomas algorithm as discussed in Carnahan et al. [11], we are found values of  $\theta$  and  $C$  for all values of  $y$  at  $t + \Delta t$ . Equation 18 and 19 are solved by same to substitute these values of  $\theta$  and  $C$ , we get solution for  $u$  and  $w$  till desired time  $t$ . calculation were execute for  $\Delta y = 0.1$ ,  $\Delta t = 0.001$  and repeated till  $y = 4$ .

### IV. RESULT AND DISCUSSION

In order to investigation, we would like to see numerical results for velocity profiles  $u$ ,  $w$ , temperature profile  $\theta$  and concentration profile  $C$  by giving numerical values of thermal Grashof number  $Gr$ , Thermophoresis or Soret number  $Sr$ , Dufour number  $Du$ , solutal Grashof number  $Gm$ , Schmidt number  $Sc$ , magnetic parameter  $M$ , Hall parameter  $m$ , permeability of porous medium  $K$ , prandtl number  $Pr$ , radiation parameter  $R$ , Eckert number  $Ec$  and inclination angle  $\lambda$  with help of graphs. As well as coefficients of skin-friction  $\tau_1$  and  $\tau_2$  along wall  $x$ -axis and  $z$ -axis, Nusselt number  $Nu$  and Sherwood number  $Sh$  are discussed through tables.

Figures 1 and 3 depict that on increasing  $Sr$ , velocity profile  $u$  and  $w$  increase and concentration  $C$  also increase while in 2, temperature profile  $\theta$  first decreases after then increases when  $Sr$  increases. velocity profiles  $u$ ,  $w$  in figure 4, temperature profile in figure 5 and concentration profile in figure 6 decrease when Schmidt number  $Sc$  increases. It is clear in figures 7 and 8 that velocity profile  $u$ ,  $w$  and temperature profile  $\theta$  decrease as Prandtl number  $Pr$  increases, on other hand concentration profile first increases after then decreases in figure 9. Figures 10 and 11 show that velocity profiles  $u$ ,  $w$  and temperature profile  $\theta$  increases when Dufour number  $Du$  increases while concentration profile  $C$  first decreases then increases in figure 12.

It is examined that velocity profiles  $u$ ,  $w$  increase when  $Gm$ ,  $Gr$ ,  $m$ ,  $K$  and  $R$  increase in figures 13, 14, 23, 16 and 17 respectively while in figure 15 velocity profile  $u$  decreases and velocity profile  $w$  increases as magnetic parameter  $M$  increases. on increasing radiation parameter  $R$ , it is analyzed that temperature profile increases in figure 18 and concentration profile decreases in figure 19. Velocity profiles  $u$ ,  $w$  decreases as inclination angle  $\lambda$  increases in figure 24. Figures 26, 27 and 28 explain that velocity profiles  $u$ ,  $w$ , temperature profile  $\theta$  and concentration profile  $C$  increase as time  $t$  increases. on increasing Eckert number  $Ec$ , in figure 20 velocity profiles  $u$ ,  $w$  increase, in figure 21 temperature profile  $\theta$  increases and in figure 22 concentration profile first decreases after then increases. Figure 25 explain that temperature profile  $\theta$  increases as  $Gr$  increases.

From table I, it is clear that on increasing Dufour number, Eckert number, inclination angle, magnetic parameter and Schmidt number, skin-friction coefficient  $\tau_1$  decreases while skin-friction coefficient  $\tau_2$  increases except inclination angle because in this case,  $\tau_2$  decreases. Further skin-friction coefficients  $\tau_1$  and  $\tau_2$  increase as Hall parameter, permeability of

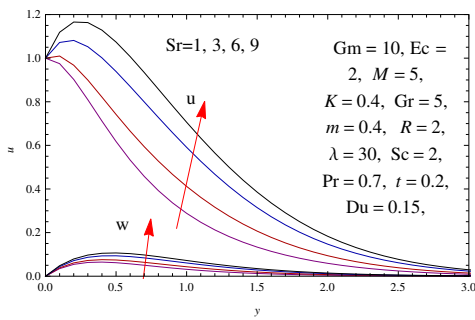


Fig. 1: Velocity Profile for Different Values of  $Sr$

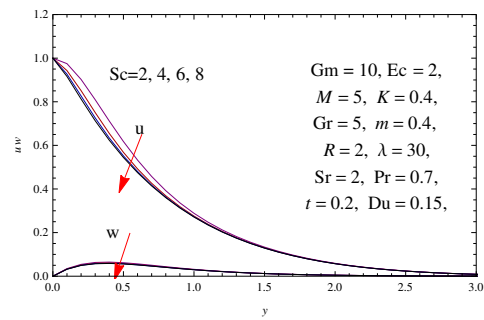


Fig. 4: Velocity Profile for Different Values of  $Sc$

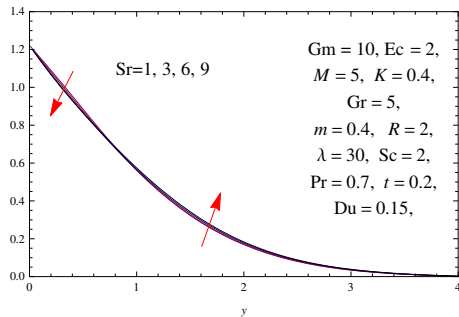


Fig. 2: Temperature Profile for Different Values of  $Sr$

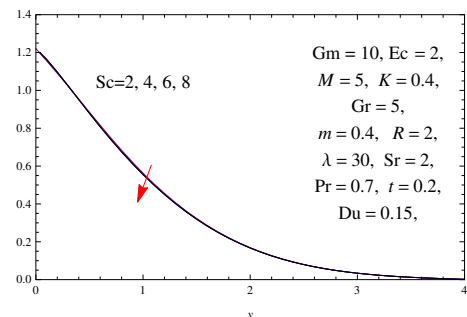


Fig. 5: Temperature Profile for Different Values of  $Sc$

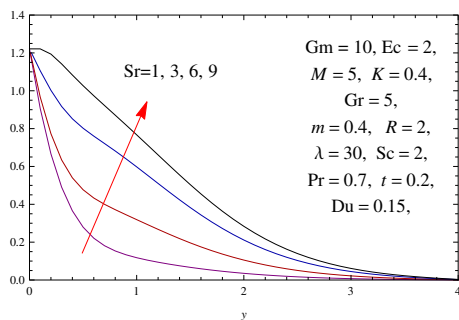


Fig. 3: Concentration Profile for Different Values of  $Sr$

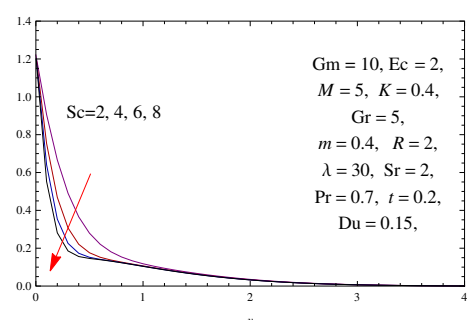


Fig. 6: Concentration Profile for Different Values of  $Sc$

porous medium and Soret number increase. In table II, we have seen that Nusselt number  $Nu$  decreases and Sherwood number  $Sh$  increases as Dufour number, Eckert number, inclination angle, magnetic parameter and Schmidt number increase. On other hand, Nusselt number increases and Sherwood number decreases when permeability of porous medium, Hall parameter and Soret number increase.

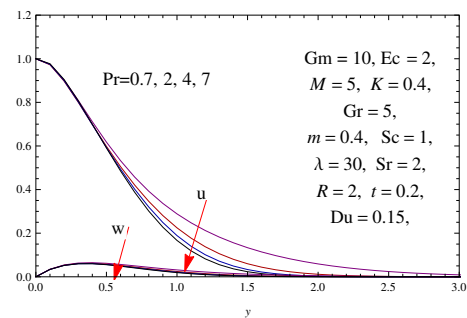


Fig. 7: Velocity Profile for Different Values of  $Pr$

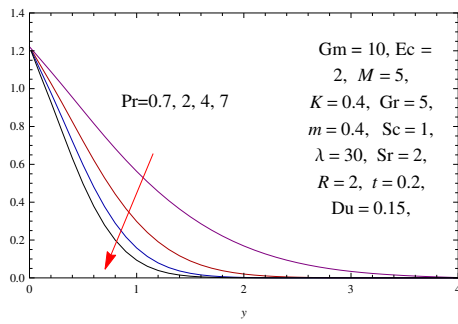


Fig. 8: Temperature Profile for Different Values of  $Pr$

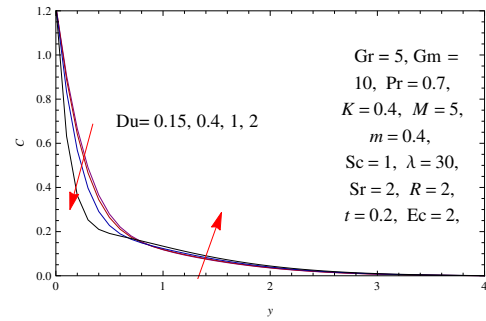


Fig. 12: Concentration Profile for Different Values of  $Du$

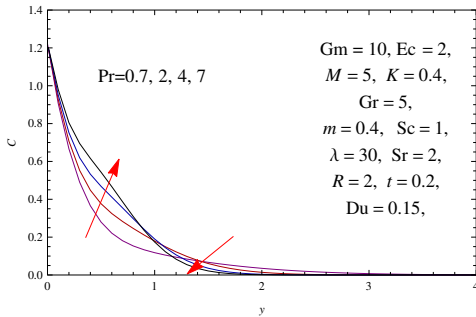


Fig. 9: Concentration Profile for Different Values of  $Pr$

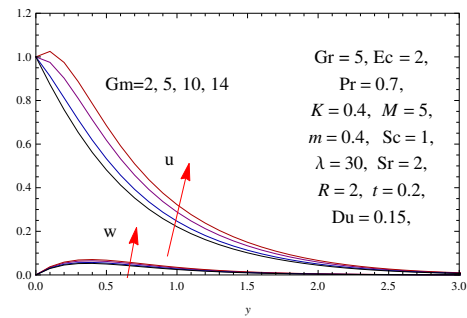


Fig. 13: Velocity Profile for Different Values of  $Gm$

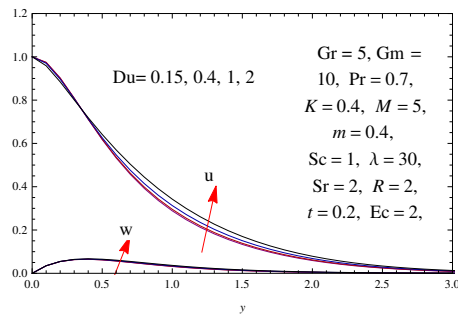


Fig. 10: Velocity Profile for Different Values of  $Du$

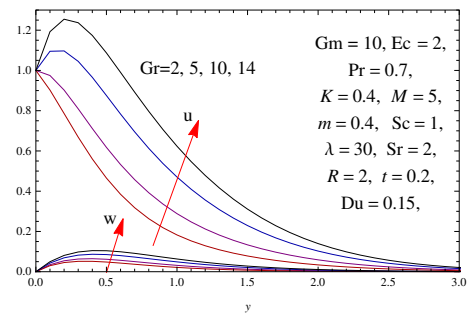


Fig. 14: Velocity Profile for Different Values of  $Gr$

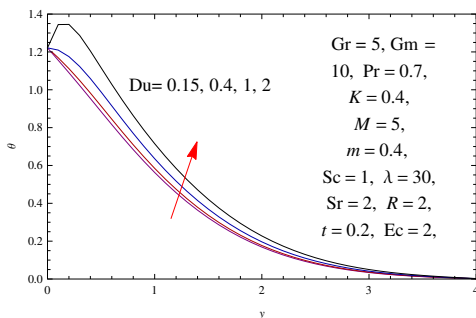


Fig. 11: Temperature Profile for Different Values of  $Du$

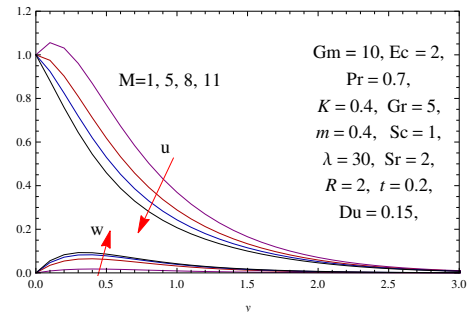


Fig. 15: Velocity Profile for Different Values of  $M$

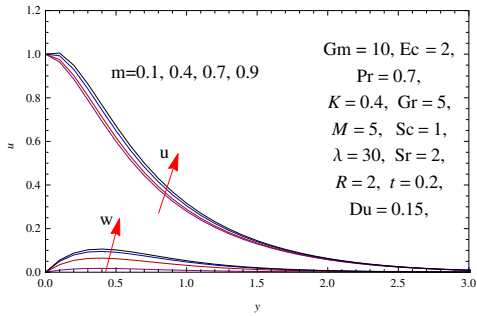


Fig. 16: Velocity Profile for Different Values of  $m$

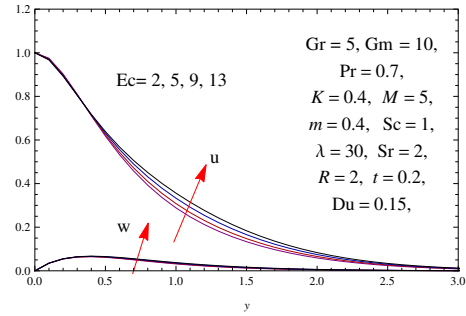


Fig. 20: Velocity Profile for Different Values of  $Ec$

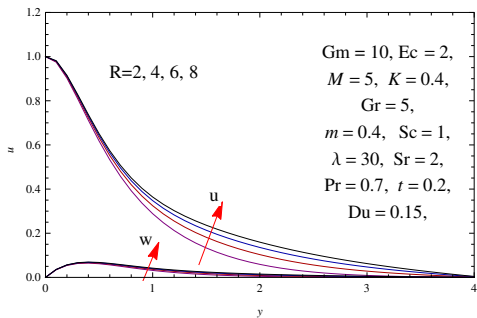


Fig. 17: Velocity Profile for Different Values of  $R$

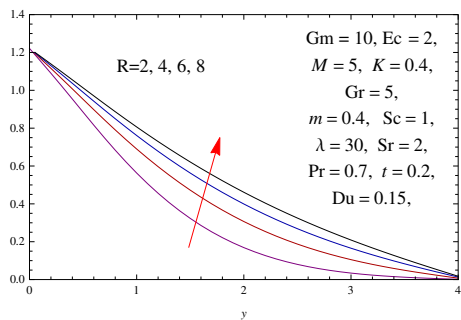


Fig. 18: Temperature Profile for Different Values of  $R$

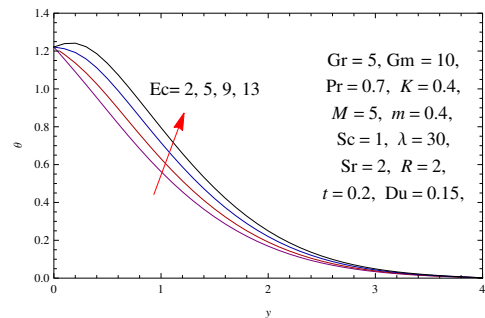


Fig. 21: Temperature Profile for Different Values of  $Ec$

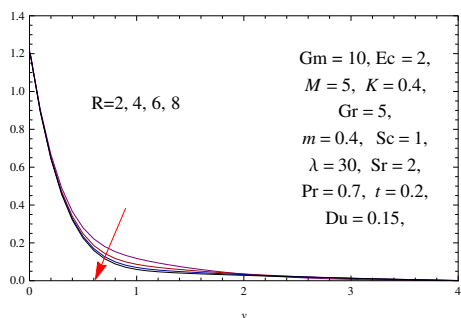


Fig. 19: Concentration Profile for Different Values of  $R$

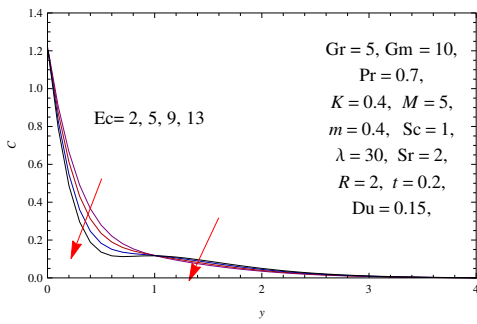


Fig. 22: Concentration Profile for Different Values of  $Ec$

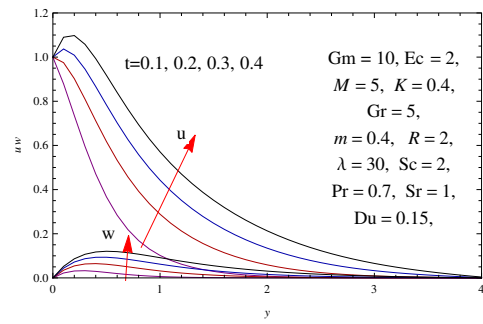


Fig. 26: Velocity Profile for Different Values of  $t$

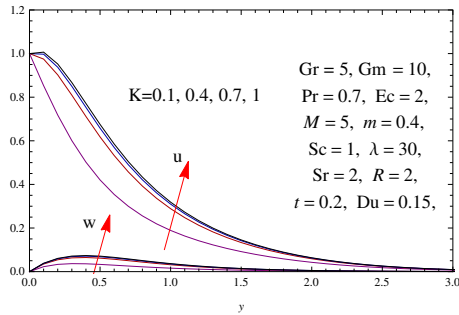


Fig. 23: Velocity Profile for Different Values of  $K$

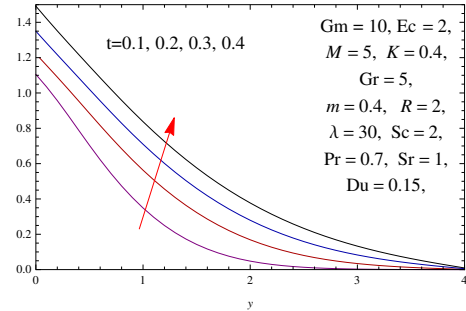


Fig. 27: Temperature Profile for Different Values of  $t$

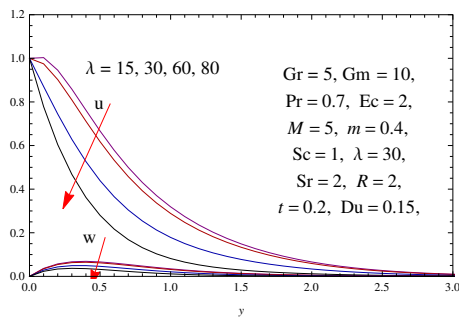


Fig. 24: Velocity Profile for Different Values of  $\lambda$

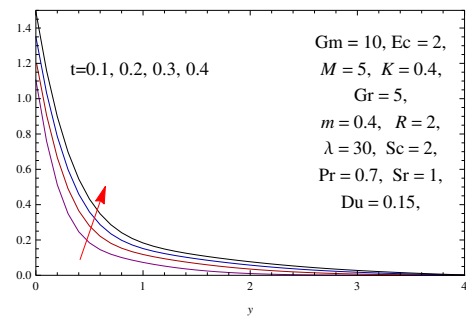


Fig. 28: Concentration Profile for Different Values of  $t$

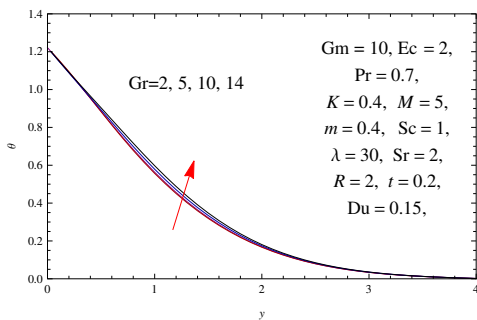


Fig. 25: Temperature Profile for Different Values of  $Gr$

ACKNOWLEDGMENT

We acknowledge the U.G.C. (University Grant Commission) India and thank for providing financial support for the research work. We are also thankful to different software companies (Mathematica, MatLab and L<sup>A</sup>T<sub>E</sub>X) for developing the techniques that help in the computation and editing.

TABLE I: Skin friction coefficients  $\tau_1$  and  $\tau_2$  for different values of parameters

$Du$	$K$	$M$	$m$	$Sc$	$Sr$	$Ec$	$\lambda$	$\tau_1$	$\tau_2$
0.4	0.4	5	0.4	2	1	2	30	-0.262354	0.348596
1	0.4	5	0.4	2	1	2	30	-0.299264	0.349403
2	0.4	5	0.4	2	1	2	30	-0.413495	0.350096
0.15	0.1	5	0.4	2	1	2	30	-1.46957	0.226897
0.15	0.7	5	0.4	2	1	2	30	-0.0284003	0.373981
0.15	1	5	0.4	2	1	2	30	0.0656808	0.385129
0.15	0.4	1	0.4	2	1	2	30	0.558337	0.0889045
0.15	0.4	8	0.4	2	1	2	30	-0.756346	0.472104
0.15	0.4	11	0.4	2	1	2	30	-1.19041	0.557969
0.15	0.4	5	0.1	2	1	2	30	-0.361406	0.0962112
0.15	0.4	5	0.7	2	1	2	30	-0.0721178	0.50398
0.15	0.4	5	0.9	2	1	2	30	0.0514978	0.555012
0.15	0.4	5	0.4	4	1	2	30	-0.569453	0.330742
0.15	0.4	5	0.4	6	1	2	30	-0.734806	0.323383
0.15	0.4	5	0.4	9	1	2	30	-0.839837	0.319297
0.15	0.4	5	0.4	2	3	2	30	0.0970871	0.385653
0.15	0.4	5	0.4	2	6	2	30	0.720037	0.441177
0.15	0.4	5	0.4	2	9	2	30	1.1883	0.481807
0.15	0.4	5	0.4	2	1	5	30	-0.274756	0.349374
0.15	0.4	5	0.4	2	1	9	30	-0.303913	0.350847
0.15	0.4	5	0.4	2	1	13	30	-0.331733	0.352234
0.15	0.4	5	0.4	2	1	2	15	0.0322543	0.36506
0.15	0.4	5	0.4	2	1	2	60	-1.29132	0.28659
0.15	0.4	5	0.4	2	1	2	80	-2.21458	0.231819

TABLE II: Nusselt number  $Nu$  and Sherwood number  $Sh$  for different values of parameters

$Du$	$K$	$M$	$m$	$Sc$	$Sr$	$Ec$	$\lambda$	$Nu$	$Sh$
0.4	0.4	5	0.4	2	1	2	30	0.522453	3.32478
1	0.4	5	0.4	2	1	2	30	0.116909	3.88489
2	0.4	5	0.4	2	1	2	30	-1.23154	5.89339
0.15	0.1	5	0.4	2	1	2	30	0.625398	3.21101
0.15	0.7	5	0.4	2	1	2	30	0.65631	3.14146
0.15	1	5	0.4	2	1	2	30	0.65716	3.13802
0.15	0.4	1	0.4	2	1	2	30	0.658741	3.12275
0.15	0.4	8	0.4	2	1	2	30	0.643005	3.17474
0.15	0.4	11	0.4	2	1	2	30	0.630966	3.19859
0.15	0.4	5	0.1	2	1	2	30	0.652411	3.15442
0.15	0.4	5	0.7	2	1	2	30	0.655268	3.14374
0.15	0.4	5	0.9	2	1	2	30	0.656306	3.13932
0.15	0.4	5	0.4	4	1	2	30	0.610945	4.67682
0.15	0.4	5	0.4	6	1	2	30	0.582103	5.80325
0.15	0.4	5	0.4	9	1	2	30	0.559975	6.68869
0.15	0.4	5	0.4	2	3	2	30	0.707304	2.54422
0.15	0.4	5	0.4	2	6	2	30	0.767936	1.1549
0.15	0.4	5	0.4	2	9	2	30	0.790856	0.000419469
0.15	0.4	5	0.4	2	1	5	30	0.399981	3.48677
0.15	0.4	5	0.4	2	1	9	30	0.0943454	3.90612
0.15	0.4	5	0.4	2	1	13	30	-0.17977	4.29576
0.15	0.4	5	0.4	2	1	2	15	0.657713	3.13826
0.15	0.4	5	0.4	2	1	2	60	0.620899	3.21343
0.15	0.4	5	0.4	2	1	2	80	0.568687	3.29447



## REFERENCES

- [1] S. Venkataramana, P. V. Satyanarayana and D. Ch. Kesavaiah, "Viscous dissipation and thermal radiation effects on unsteady MHD convection flow past a semi infinite vertical permeable moving plate", *Int. J. of Appl. Math.*, pp. 476-487, 2011.
- [2] E. M. Sparrow and R. D. Cess, "Effect of magnetic field on free convection heat transfer", *Int. J. Heat and Mass Transfer*, vol. 3, pp. 267-270, 1961.
- [3] A. Postelnicu, "Influence of magnetic field on heat and mass transfer by natural convection from vertical surface in porous media considering Soret and Dufour effects", *Int. J. Heat and Mass Transfer*, vol. 47, no. 67, pp. 1467-1472, 2004.
- [4] Rajesh and Vijay Kumar Verma, "Radiation and mass transfer effects on MHD free convection flow past an exponentially accelerated vertical plate with variable temperature", *ARPJ J. of Eng. and Appl. Sci.*, vol. 4, no. 6, pp. 20-26, 2009.
- [5] A. R. Bestman, M. .A. Alabraba and A. ogulu, "Laminar convection in binary mixed of hydro magnetic flow with radiative heat transfer", *Astrophysics and Space Science*, vol. 195, no. 2, pp. 431-439, 1992.
- [6] Olanrewaju Philip dadapo, "Dufour and Soret effects of a transient free convective flow with radiative heat transfer past a flat plate moving through a binary mixture", *Pacific J. of Sci. and Tech.*, vol. 11, no. 1, 2010.
- [7] A. Sudha Karraiah, D. Kesaraiah Chenna and M. Bhavana, "The Soret effect on free convective unsteady MHD flow over a vertical plate with heat source", *Int. J. of innovative R. in Sci. Eng. and Tech.*, vol. 2, no. 5, pp. 1617-1628, 2013.
- [8] S. K. Ghosh, "Effects of Hall current on MHD Couette flow in a rotating system with arbitrary magnetic field", *Czech. J. Phys.*, vol. 2, no. 1, pp. 51-63, 2002.
- [9] R. N. Jana and A. K. Kanch, "Hall effect on unsteady Couette flow under boundary layer approximation", *J. Physical Sci.*, vol. 7, pp. 74-86, 2001.
- [10] T. G. Cowling, *Magnetohydrodynamics*, Inter Science Publishers, New York, 1957.
- [11] Brice Carnahan, H. A. Luthor and J. O. Wilkes, *Applied Numerical Methods*, John Wiley and Sons, New York, 1969.